Polymer 51 (2010) 2376–2382

Contents lists available at ScienceDirect

Polymer

journal homepage: www.elsevier.com/locate/polymer

A simple method for creating nanoporous block-copolymer thin films

Wonjoo Lee, Xin Zhang, R.M. Briber*

Department of Materials Science and Engineering, University of Maryland, College Park, MD 20742-2115, USA

ARTICLE INFO

Article history:
Received 14 January 2010
Received in revised form
10 March 2010
Accepted 13 March 2010
Available online 27 March 2010

Keywords:
Nanopore
Block copolymer phase separation
Anti-reflection coating

ABSTRACT

We introduce a simple method to create block copolymer films with controlled porosity. We show that the pore structure can be varied over a broad range of length scales not obtainable in homopolymer blend films. The morphology is a random two phase kinetically trapped structure that is not limited by the equilibrium block copolymer structure. The morphology is obtained through blending homopolymer poly(4-vinylpyridine) (P4VP) with block copolymer polystyrene-b-poly(4-vinylpyridine) (PS-b-P4VP) and then removing the homopolymer P4VP by washing with ethanol. The structure obtained prior to washing (which templates the nanoporous structure) is stabilized in the kinetically trapped morphology during spincoating and is not obtainable from either homopolymer blends or the pure block copolymer. When PS/P4VP blend solutions in tetrahydrofuran were spincoated at 25% relative humidity, continuous films with raised P4VP nanodomains were formed due to a preferential affinity of the spinning solvent for polystyrene. In a similar manner, when PS-b-P4VP/P4VP block copolymer/homopolymer solutions were spincoated, the P4VP homopolymer was solubilized in the P4VP block domains during spincoating, suppressing macro-phase separation. The film morphology is generated at the air surface and then propagates through the film, resulting in P4VP nanodomains oriented vertically to the substrate. In the resulting films, the size of P4VP nanodomains were varied by increasing the amount of P4VP homopolymer. The subsequent extraction of P4VP homopolymer from the PS-b-P4VP/P4VP blend films in ethanol resulted in nanopores with a distribution of length scales. The morphology of these materials makes the films potentially suitable for a range of applications such as anti-reflective coatings, nanoporous membranes and low-k materials. An illustrative example of an anti-reflective coating will be presented.

1. Introduction

Light reflection from the surface of optical components is generally undesirable, disrupting and degrading the performance of optical and display devices fabricated from glass-based optical materials. Anti-reflection (AR) coatings are used to reduce the intensity of reflection and produce highly transmissive optical components. Reflections are suppressed at wavelengths near the quarter-wavelength optical thickness when the square of n_f is equal to the product of n_o and n_s, where n_f , n_o and n_s represent the refractive indices of film, air and substrate, respectively [1–3]. As optical elements based on glass and common transparent plastic substrates have refractive indices in the range of 1.45–1.7, n_f must be between 1.2 and 1.3 for efficient AR coatings, which is not readily available as the lowest refractive indices for dielectrics are on the order of 1.35. One approach to solve the problem is to use a nanoporous film instead of a homogeneous layer. Methods to construct nanoporous films have been developed including patterned surfaces [4], sol–gel processes [5], polyelectrolyte multilayers [6], vapor deposition [7], and phase separation with selective dissolution [3]. Among those, phase separation of binary blends of mutually incompatible polymers during spincoating, and subsequent removal of one of the polymer components is a simple, fast, and reliable method to generate nanopores in the remaining film [3]. However, because the dimensions of the pores are determined by the phase separation time of the two polymer components, the pore size is difficult to control. Block copolymers are well-known to self-assemble into nano- and meso-scale structures and the use of block copolymers for nanostructured patterns has attracted increasing attention due to their potential use as templates and scaffolds for the fabrication of functional nanostructures [8–11]. It is possible to generate nanoporous films with a controlled nanopore size by removing homopolymer from block copolymer/homopolymer blend films [12–14] or a low molecular additive from a block copolymer/additive film [15]. The resultant nanopores are templated by the equilibrium block copolymer morphology through thermal annealing or solvent annealing. The nanopore size can be

* Corresponding author. Tel.: +1 301 405 5207; fax: +1 301 314 2029.
E-mail address: rbriber@umd.edu (R.M. Briber).

0032-3861/$ – see front matter © 2010 Elsevier Ltd. All rights reserved.
doi:10.1016/j.polymer.2010.03.023

further enlarged by completely eliminating one of the blocks [13]. For these cases, numerous processing steps are generally required and the pore size distribution is relatively narrow and determined by the maximum amount of loaded homopolymer or additive as the equilibrium morphology is governed by the thermodynamic phase diagram. In this work, we have adopted a strategy to generate nanopores oriented normal to the substrate in thin block copolymer films using polystyrene-b-poly(4-vinylpyridine) block copolymer (PS-b-P4VP) and poly(4-vinylpyridine) (P4VP) homopolymer blends spun from tetrahydrofuran (THF) solutions, where THF has a preferential affinity for PS. Although it is possible to regulate the size or order of nanopores in PS-b-P4VP/P4VP films through solvent annealing, here we will focus on the phase separation behavior of the PS-b-P4VP/P4VP blends during spincoating since P4VP homopolymers are solubilized in the P4VP blocks without macro-phase separation under our experimental conditions. This enabled us to control the pore size after the extraction of P4VP homopolymer from the film, resulting in a simple rapid method to control the structure of the nanoporous films.

2. Experimental

PS-b-P4VP (number average molecular weight M_n^{PS} = 310 kg mol^{-1}, M_n^{P4VP} = 10 kg mol^{-1}, polydispersity index = 1.09), PS homopolymer (M_n = 300 kgmol^{-1}, polydispersity index = 1.2) and P4VP homopolymer (M_n = 5.1 kgmol^{-1}, polydispersity index = 1.06) were purchased from Polymer Source, Inc., and used without further purification. PS/P4VP and PS-b-P4VP/P4VP were dissolved in THF from Aldrich at 80 °C for 12 h and cooled to room temperature. In the resulting solutions, the concentration of PS or PS-b-P4VP was fixed at 0.5 wt%, but the concentration of P4VP homopolymer was changed and, depending on the amount of P4VP homopolymer added, the P4VP weight fraction varied from 0.03 to 0.55. Here, P4VP weight fraction is defined by the ratio of the total P4VP weight (P4VP homopolymer and P4VP block) to the total polymer weight in the solutions. The polymer solutions were prefiltered through Millipore 0.45 μm poly(tetrafluoroethylene) filters. PS/P4VP and PS-b-P4VP/P4VP blend films were prepared by spincoating at 3000 rpm for 60 s on silicon substrates, mica, or glass slides. The surface morphology of as-spun PS/P4VP or PS-b-P4VP/P4VP blend films on silicon substrates was characterized using a Dimension 3000 atomic force microscope (AFM) from Digital Instruments, Inc. Silicon tips on a cantilever with spring constants ranging between 20.0 and 80.0 Nm (as specified by the manufacturer) were used. To measure thin film thickness, the polymer films deposited on silicon substrates were scratched with a scalpel, and AFM images were taken at the borders of the scratches. Transmission electron microscopy (TEM) was performed using a JEOL JEM-2100F field emission TEM at 200 kV coupled with a Gatan CCD camera. TEM samples were spun on mica with the same conditions described before, floated on deionized water, captured on a TEM grid, and stained with iodine. To prepare nanoporous films, as-spun PS-b-P4VP/P4VP blend films were soaked in ethanol, which is a highly selective solvent for P4VP, and dried in air. In order to confirm whether nanopores penetrate through the film, the tilted image of a PS-b-P4VP/P4VP blend film with 0.55 of P4VP weight fraction was observed using scanning electron microscopy (SEM). A layer of gold was coated on the surface of a nanoporous block-copolymer film and then the film was cleaved in liquid nitrogen to preserve the morphology. SEM observation was conducted using a Hitachi SU-70 Schottky field emission gun SEM working at 3 kV accelerating voltage and working distance of 6 mm. Transmittance of a glass slide with a nanoporous PS-b-P4VP film was measured using a Perkin–Elmer Lambda 25 UV/Vis spectrometer and was compared to a bare glass slide.

3. Results

It has been reported in the review paper by H. Colfen that P4VP is difficult to polymerize anionically due to insolubility in THF above a critical molecular weight [16]. For PS-b-P4VP block copolymers with P4VP weight fraction above 0.16, spherical PS-b-P4VP micelles in THF were observed using static and dynamic light scattering [17]. Recently, in the work by Ali and Park, PS-b-P4VP block copolymers (12 kgmol^{-1}-b-11.8 kgmol^{-1} and 3.3 kgmol^{-1}-b-18.7 kgmol^{-1}) in a toluene/THF mixture, which have a smaller M_n^{PS} and a similar M_n^{P4VP} compared to our PS-b-P4VP block copolymer, were studied using small angle X-ray scattering to investigate the effects of solvent selectivity and block copolymer composition on the micellar structure [18]. Ali and Park found that PS-b-P4VP formed micelles only in a mixture of toluene/THF because toluene is a selective solvent for PS and THF is non-selective due to the small M_n^{P4VP}. Our PS/P4VP and PS-b-P4VP/P4VP polymer solutions in THF are optically transparent indicating that no large aggregates are formed due to the low P4VP weight fraction (~0.03) and the small M_n^{P4VP}. Also, the 5.1 kgmol^{-1} P4VP homopolymer used here completely dissolved in THF even at room temperature as the M_n is relatively small. Fig. 1(a) is an AFM height image (2 μm × 2 μm scale) of an as-spun PS/P4VP homopolymer blend film on a silicon substrate spun from a 0.5 wt% PS solution in THF with 0.35 of P4VP weight fraction. The AFM image shows that nodules protrude an average 10 nm height above a continuous matrix. Similar morphologies have been observed in various homopolymer blend films by other researchers [19–23]. The morphology is formed due to the rapid quench by solvent evaporation. Initially, PS and P4VP are dissolved in THF, and during spincoating, the THF evaporates and phase separation of PS and P4VP occurs. Since THF is a better solvent for PS compared to P4VP (as indicated by the reported Flory–Huggins interaction parameters $\chi_{PS\text{-}THF}$=0.35 and $\chi_{P4VP\text{-}THF}$=0.6) [24], P4VP-rich phases are more quickly depleted of solvent and solidify earlier. Subsequent evaporation of the remaining solvent leads to a collapse of the PS-rich phase, and results in elevated P4VP nodules. It was confirmed that the morphology can be used to generate nanopores, which resemble the nodules in size and shape, by selectively dissolving the P4VP homopolymer in ethanol, as shown in Fig. 1(b).

For a broad-band AR coating, the volume ratio of pores should be maximized while nanopores are much smaller than the wavelength of light for limited light scattering from the pores. It is desirable to have a system where the morphology is reproducible and readily scaled to different pore sizes. To achieve this, the system was extended to PS-b-P4VP block copolymer/P4VP homopolymer blends. The goal was not to produce a highly ordered block copolymer structure but to produce two phase random morphologies where the pore size was easily varied using simple processing technique. To control the pore size, the amount of P4VP homopolymer was varied in the PS-b-P4VP/P4VP blend. As the concentration of P4VP homopolymer in the polymer solutions increases, the film thickness of the as-spun films increased from 25 nm to 60 nm. Fig. 2(a)–(e) show AFM height images of as-spun PS-b-P4VP/P4VP blend films as a function of P4VP weight fraction. Although the PS-b-P4VP film without P4VP homopolymer in Fig. 2 (a) has a weight fraction of about 0.03 of P4VP, the film showed a self-assembled structure with P4VP domains in the PS matrix due to the strong repulsive interaction between the PS and the P4VP blocks. The reported Flory–Huggins interaction parameter, χ, of PS-b-P4VP is approximately an order of magnitude greater than the largest values of reported χ in other nonionic systems [25], which is corroborated by block copolymer order–disorder transition temperatures well above 300 °C [26]. P4VP weight fraction in PS-b-P4VP/P4VP films was increased up to 0.55 by adding P4VP

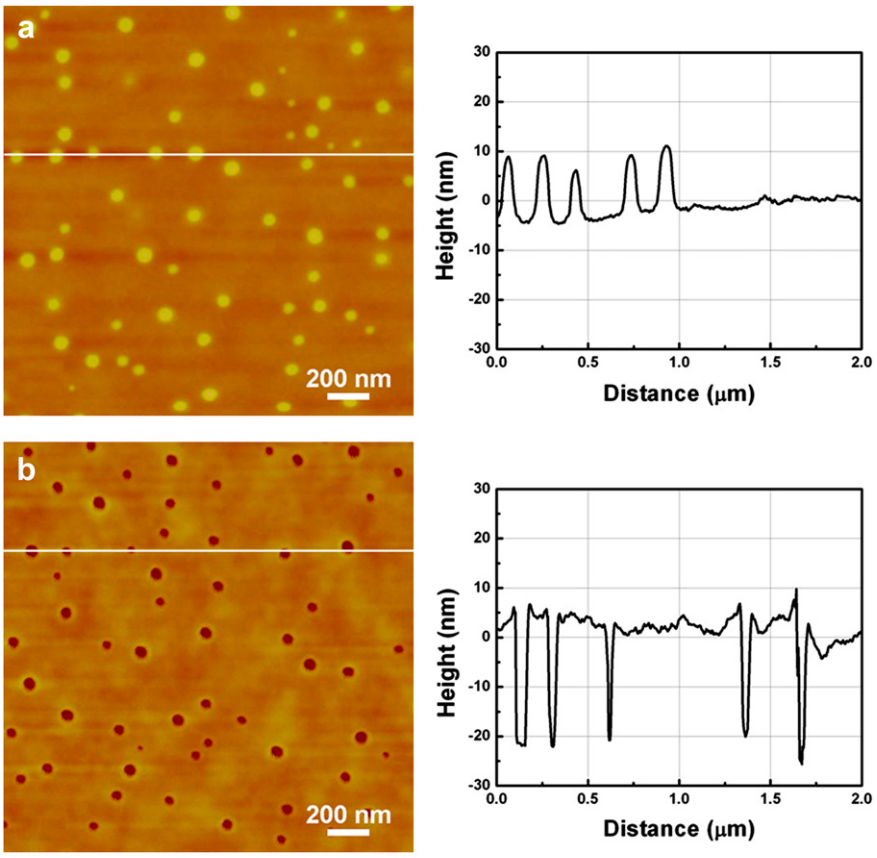

Fig. 1. AFM height images of (a) an as-spun PS/P4VP blend film with 0.35 of P4VP weight fraction and (b) the PS/P4VP blend film after immersed in ethanol.

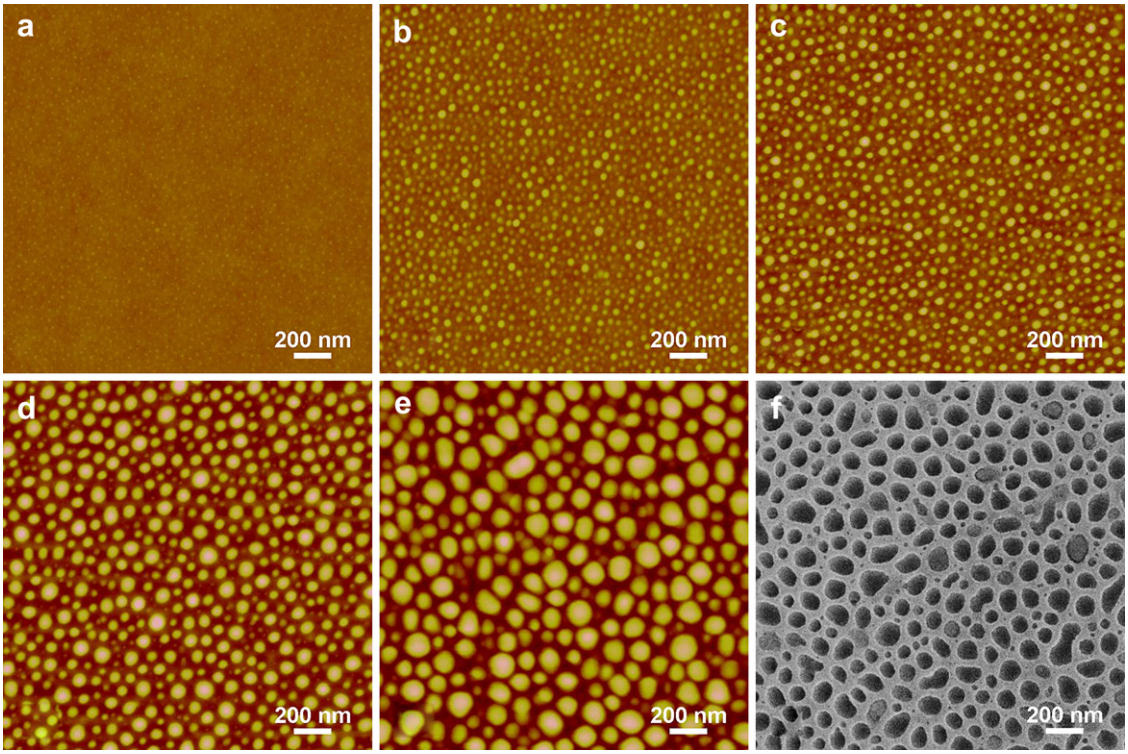

Fig. 2. AFM height images of as-spun PS-b-P4VP/P4VP blend films as a function of P4VP weight fraction in the polymer solutions. P4VP weight fraction in the solutions was (a) 0.03, (b) 0.25, (c) 0.34, (d) 0.45, and (e) 0.55. (f) A TEM image of PS-b-P4VP/P4VP film with 0.55 of P4VP weight fraction after iodine staining.

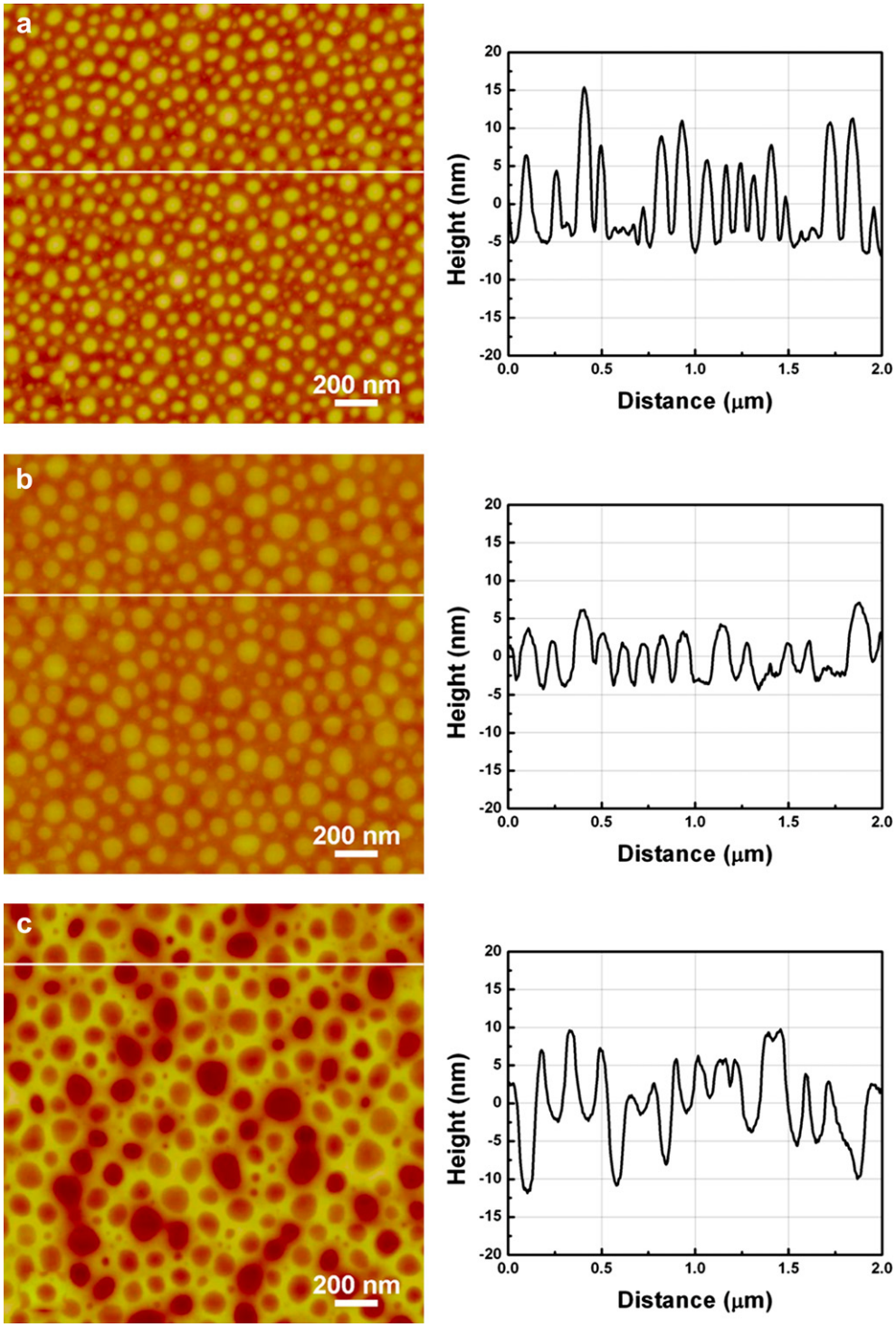

Fig. 3. AFM height images of as-spun PS-b-P4VP/P4VP blend films with 0.45 of P4VP weight fraction as a function of relative humidity (RH). RH: (a) 25%, (b) 40%, and (c) 60%.

homopolymer to the PS-b-P4VP solutions in THF. As the P4VP weight fraction in the polymer solutions increases, larger nodules are observed in the as-spun films, as shown in Fig. 2(b)–(e). In contrast to the PS/P4VP homopolymer blend film (Fig. 1(a)), the nodules are more evenly and closely distributed throughout the films. A bi-continuous structure, which has been observed by Li et al. when the weight fraction of P4VP in a PS/P4VP blend film is about 0.5 [21] was not observed in these films. TEM was used to identify the P4VP domains in a PS-b-P4VP/P4VP film with 0.55 of P4VP weight fraction after iodine staining.

Since iodine selectively stains the P4VP polymer, the P4VP domains appear darker in the TEM image shown in Fig. 2(f). The size and shape of nodules in the AFM image of (e) film is comparable to those of darker domains in the TEM image of (f). These observations indicate that the P4VP homopolymer is solubilized in P4VP block domains during spincoating.

It can be argued that the observed morphology of PS-b-P4VP/P4VP blend films is similar to that of reported PS-b-P4VP micelle films [27]. To verify that nodular P4VP domains in PS-b-P4VP/P4VP blend films are formed due to the preferential affinity of THF for PS, similar to the blend films, and not due to micelles in solution we spincoated a PS-b-P4VP/P4VP solution with 0.45 of P4VP weight fraction at different levels of relative humidity (RH). RH during spincoating was controlled by adding water vapor to a glass chamber enclosing the spinning chuck on which the substrate was placed. RH was measured with a hydrometer inside the glass chamber. Fig. 3 shows AFM height images of as-spun films as a function of RH. For clarity, all three images are set to the same height scale (30 nm). When the RH increased from 25% to 40% during spincoating, the height of the domains decreased. At 60% RH, the protruding nodular domains changed into pits. The observed behavior is related to breath figure formation although breath figure occurs at microscale [28]. Generally, breath figures are ascribed to solvent-evaporative cooling on the surface of a polymer solution under humid conditions where water vapor is condensed into water droplets at the solution surface. The water droplets then interact with each other and become hexagonally packed. After complete evaporation of the solvent and water, traces of water droplets remain as a honeycomb structure in the polymer film. In our case, the fact that nodular domains, generated under dry conditions, were changed into pits under humid conditions indicates that THF evaporation rate was altered in the P4VP domains under humid conditions and since THF evaporates faster in the P4VP domains than in the PS matrix, this difference will cause the water vapor to condense preferentially on the P4VP domains.

The condensed water will significantly lower the THF evaporation rate from the P4VP domains and lead to an elevated PS matrix since P4VP domains solidify last after the complete evaporation of the THF and condensed water. As our films consist of two components (PS-b-P4VP block copolymer and P4VP homopolymer), the morphology obtained at humid conditions is still irregular. The variation of the structure with RH indicates that the morphology of the film is not formed from micelle present in the spinning solution. In addition variation of RH allows for secondary control of domain size and structure at a fixed PS-b-P4VP/P4VP composition.

Mean field calculations have shown that hexagonally packed P4VP cylinders embedded in PS can be expected for a volume fraction of P4VP block ranging from 0.12 to 0.31 [29,30]. Therefore, as the concentration of added P4VP homopolymer increases, it might be expected that the PS-b-P4VP/P4VP blend films transition between sphere, cylinder and lamellar morphologies. Generally, in block copolymer melts, the morphology of the equilibrium microstructure is dependent on the volume fraction of minority block, the degree of polymerization and χ between the blocks [8]. However, in block copolymer solutions, the phase behavior is more complicated and also depends on the polymer–solvent interaction parameters and the volume fraction of the polymer in the solution. During spincoating process, the solvent evaporates and the concentration of polymer solution varies from dilute to concentrated before formation of a thin film. Additionally, in our case, THF evaporates at different rates from the PS-rich phase compared to the P4VP-rich phase, due to the preferential affinity to the solvent. Therefore, the observed self-assembled structures of PS-b-P4VP/P4VP blend films, fabricated through spincoating, are far from thermodynamic equilibrium. It is important to emphasize that the structures shown in Fig. 2 are morphologies with a high area fraction of dispersed phase that is in a trapped non-equilibrium state. This morphology is generated through the use of a block copolymer blended with a homopolymer but purposely does not attempt to generate a classical microphase-separated equilibrium block copolymer morphology. The presence of the block copolymer

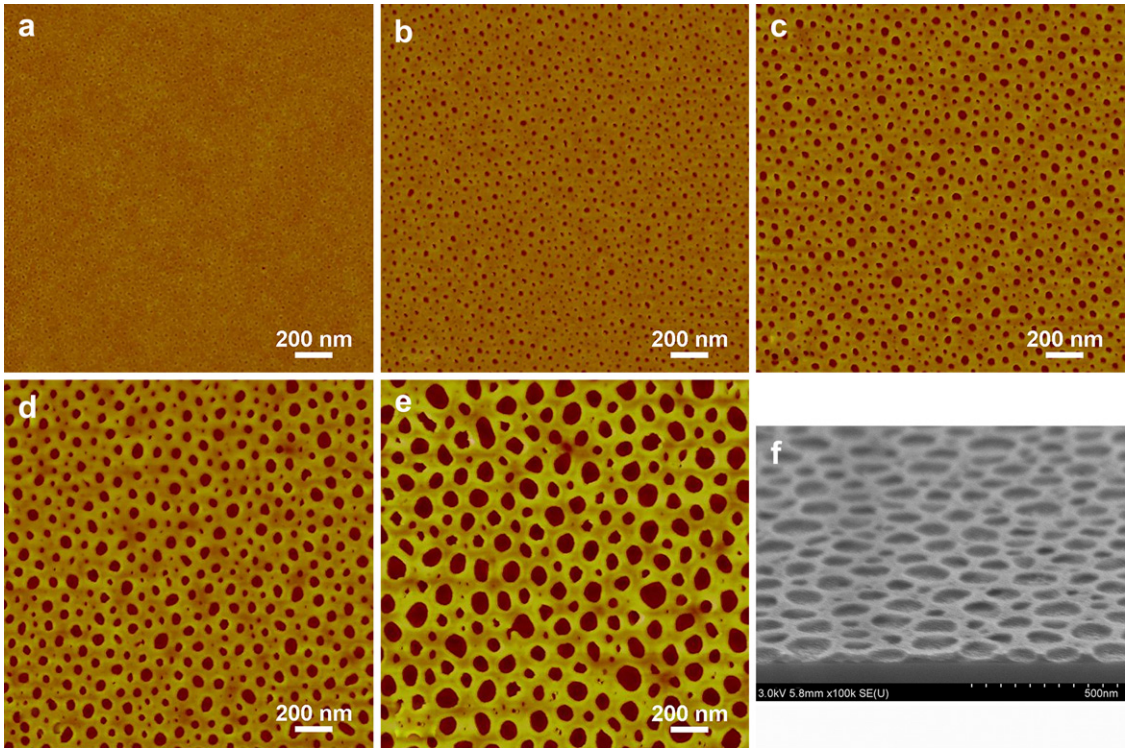

Fig. 4. AFM height images of PS-b-P4VP/P4VP blend films after soaked in ethanol. P4VP weight fraction in the polymer solutions was (a) 0.03, (b) 0.25, (c) 0.34, (d) 0.45, and (e) 0.55. (f) A SEM tilted image of the film (e).

provides access and control over morphologies with length scales and structures that would be difficult to obtain with homopolymer blends.

In addition this morphology can be scaled by varying the homopolymer volume fraction. In the next section it will be demonstrated that these morphologies form a natural template for creating nanoporous films. To convert the self-assembled structure to a nanoporous morphology, the P4VP homopolymer was removed by soaking in ethanol. Resultant pore diameter increased with increasing P4VP homopolymer concentration, as shown in Fig. 4(b)–(e). When a PS-b-P4VP film without P4VP homopolymer was soaked in ethanol, the nodules changed into pits (Fig. 4(a)), which is in agreement with the work of Russell et al. where they found that PS-b-P4VP films, fabricated through spincoating of PS-b-P4VP solutions from toluene/THF, undergo surface reconstruction after soaking in ethanol, producing nanopores in the film [31,32]. To check whether the nanopores propagate through the film, the films were observed by SEM. Fig. 4(f) shows a SEM image of a film with 0.55 P4VP weight fraction which was thickest film studied. The pores are vertical to the substrate which indicates that the self-assembly starts at the air surface and then propagates through the film to the substrate under these conditions. In addition films were removed from the substrate and the structure on the backside of the film was observed by AFM. Pores were seen to have traversed the thickness of the film.

Fig. 5(a) shows a plot of average pore diameter and pore fraction versus P4VP weight fraction, calculated from the AFM data using ImageJ program [33]. As P4VP weight fraction increases, the average pore diameter increases from 10 nm to 72 nm and the standard deviation increases due to an increase in the width of the pore size distribution. The width of the pore size distribution increases with increasing volume fraction of P4VP homopolymer. It may be possible to control the pore size distribution through varying of the molecular weight of the copolymer blocks and/or homopolymer but this is beyond the scope of this paper. Because the largest pore diameter in the film (e) in Fig. 4 is still smaller than 200 nm despite the larger standard deviation, the nanoporous film did not cause visible light scattering. The pore fraction also increases as P4VP weight fraction increases although the calculated values are lower than the expected porosity as the P4VP domains are thicker than the continuous PS matrix and the P4VP homopolymer that is elevated above the matrix does not contribute to the generation of pores. The effective refractive index (n_f) of the nanoporous film will decrease as the pore fraction increases and can be estimated using the following equation: [34]

$$n_f^2 = \sum_i v_i n_i^2$$

where n_i and v_i are the refractive indices and the volume fractions of pore and polymer, respectively. Using a refractive index of PS-b-P4VP (1.59) [15] at 632.8 nm, the calculated effective refractive index of the nanoporous film decreases from 1.56 to 1.43 as the P4VP weight fraction increases. Transmittance of a glass slide with the nanoporous film (e) in Fig. 4 (having the lowest refractive index among the films) on both sides was measured and compared to a bare glass slide. The coated glass slide shows lower reflectivity in the measured wavelength range, demonstrating possible use as an AR coating. Although the average transmittance for visible light was increased from 90% to 94.2%, it is still lower than the value obtained using 106 nm thick poly(methyl methacrylate) nanoporous films reported by Walheim et al. [3].

Aside from the lower porosity in the films compared to the expected porosity, one possible reason may be due to the thickness (d) of our film (60 nm) and that the wavelength maximum (λ_{max}) of

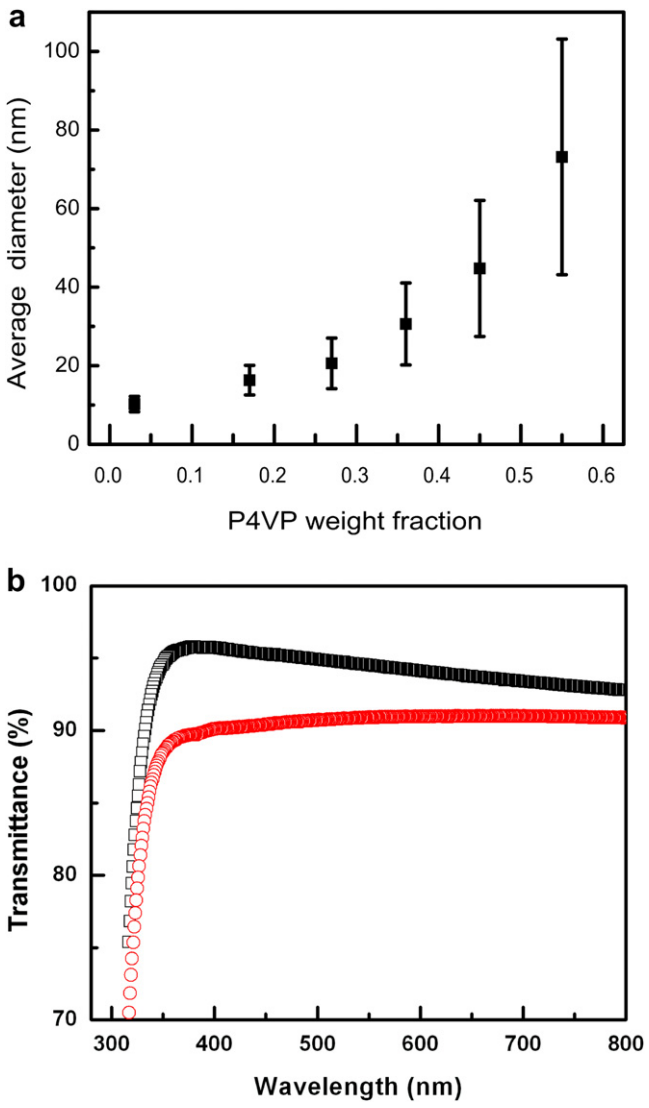

Fig. 5. (a) A plot of average pore diameter (closed squares) and porosity (open squares) versus P4VP weight fraction and (b) transmittance of a glass slide with the nanoporous film (e) on both sides (black squares) and a bare glass slide (red circles).

the transmittance increases linearly with the film thickness ($\lambda_{max} = 4nd$) [3]. Although the film thickness is easily adjusted by varying the spincoating speed or the polymer solution concentration, the relatively poor mechanical properties of such polymer films would probably need to be improved for practical applications using polymer-inorganic particle hybrid materials. In addition it may be possible to prepare gradient hybrid films to improve on the anti-reflective properties of the films. However, it is emphasized that we are presenting a simple method to suppress macro-phase separation by solubilizing homopolymer in one block of a block copolymer and subsequently controlling porosity by removing the homopolymers by washing with a selective solvent. This technique can be used as an underlying principle for preparing AR coatings.

4. Conclusions

We have demonstrated that using the preferential solubility of PS in THF compared to P4VP, self-assembled structures can be generated in both PS/P4VP and PS-b-P4VP/P4VP blend films. In the resulting films, P4VP domains protruded from the surface and their

size was easily controlled by regulating the amount of P4VP homopolymer. It is noteworthy that in our method, macro-phase separation was suppressed as the added P4VP homopolymer was solubilized in P4VP block of the copolymer during spincoating. The morphologies generated are non-equilibrium and are kinetically trapped during spincoating. These morphologies are highly reproducible and represent a simple method to form nanoscale structures not easily produced by other methods and which can readily template nanoporous materials. Due to the large incompatibility of PS and P4VP, the added P4VP homopolymer was readily extracted from the as-spun films with the environmentally benign solvent, ethanol, resulting in multiple length scale nanopores in the corresponding films. As the generated nanopore diameters are smaller than the wavelength of visible light, the nanoporous film has the potential to be used for AR coatings, nanoporous membranes or low-k material. An illustrative example of their use as an AR coating has been provided.

Acknowledgement

We acknowledge the support of the Maryland NanoCenter and its NISPLab. The NISPLab is supported in part by the NSF as a MRSEC Shared Experimental Facility. Funding is acknowledged from the Department of Commerce through the National Institute of Standards and Technology.

References

[1] Hiller JA, Mendelsohn JD, Rubner MF. Nature Materials 2002;1(1):59–63.
[2] Ibn-Elhaj M, Schadt M. Nature 2001;410(6830):796.
[3] Walheim S, Schaffer E, Mlynek J, Steiner U. Science 1999;283(5401):520–2.
[4] Heine C, Morf RH. Applied Optics 1995;34(14):2476–82.
[5] Uhlmann DR, Suratwala T, Davidson K, Boulton JM, Teowee G. Journal of Non-Crystalline Solids 1997;218:113–22.
[6] Hattori H. Advanced Materials 2001;13(1):51–4.
[7] Neuman GA. Journal of Non-Crystalline Solids 1997;218:92–9.
[8] Bates FS, Fredrickson GH. Annual Review of Physical Chemistry 1990;41:525–57.
[9] Lazzari M, MAL-Q. Advanced Materials 2003;15(19):1583–94.
[10] Park C, Yoon J, Thomas EL. Polymer 2003;44(22):6725–60.
[11] Thurn-Albrecht T, Schotter J, Kastle CA, Emley N, Shibauchi T, Krusin-Elbaum L, et al. Science 2000;290(5499):2126–9.
[12] Jeong U, Ryu DY, Kho DH, Lee DH, Kim JK, Russell TP. Macromolecules 2003;36(10):3626–34.
[13] Jeong U, Ryu DY, Kim JK, Kim DH, Wu X, Russell TP. Macromolecules 2003;36(26):10126–9.
[14] Kim SH, Misner MJ, Russell TP. Advanced Materials 2004;16(23–24):2119–23.
[15] Sidorenko A, Tokarev I, Minko S, Stamm M. Journal of the American Chemical Society 2003;125(40):12211–6.
[16] Colfen H. Macromolecular Rapid Communications 2001;22(4):219–52.
[17] Antonietti M, Heinz S, Schmidt M, Rosenauer C. Macromolecules 1994;27(12):3276–81.
[18] Ali N, Park S-Y. Langmuir 2008;24(17):9279–85.
[19] Boltau M, Walheim S, Mlynek J, Krausch G, Steiner U. Nature 1998;391(6670):877–9.
[20] Cui L, Peng J, Ding Y, Li X, Han Y. Polymer 2005;46(14):5334–40.
[21] Li X, Xing R, Zhang Y, Han Y, An L. Polymer 2004;45(5):1637–46.
[22] Tanaka K, Takahara A, Kajiyama T. Macromolecules 1996;29(9):3232–9.
[23] Walheim S, Boltau M, Mlynek J, Krausch G, Steiner U. Macromolecules 1997;30(17):4995–5003.
[24] Park S, Wang J-Y, Kim B, Chen W, Russell TP. Macromolecules 2007;40(25):9059–63.
[25] Clarke CJ, Eisenberg A, La Scala J, Rafailovich MH, Sokolov J, Li Z, et al. Macromolecules 1997;30(14):4184–8.
[26] Zha W, Han CD, Lee DH, Han SH, Kim JK, Kang JH, et al. Macromolecules 2007;40(6):2109–19.
[27] Kim B, Park S, McCarthy TJ, Russell TP. Small 2007;3(11):1869–72.
[28] Srinivasarao M, Collings D, Philips A, Patel S. Science 2001;292:79–83.
[29] Peinemann K-V, Abetz V, Simon PFW. Nature Materials 2007;6(12):992–6.
[30] Matsen MW, Bates FS. Macromolecules 1996;29(4):1091–8.
[31] Park S, Kim B, Wang JY, Russell TP. Advanced Materials 2008;20(4):681–5.
[32] Park S, Wang J-Y, Kim B, Russell TP. Nano Letters 2008;8(6):1667–72.
[33] Abramoff MD, Magelhaes PJ, Ram SJ. Biophotonics International 2004;11(7):36–42.
[34] Wedgewood AR, Seferis JC. Polymer Engineering and Science 1984;24(5):328–44.